J. Biochem. 129, 477–484 (2001)

Cold Adaptation of the Thermophilic Enzyme 3-Isopropylmalate Dehydrogenase[1]

Masako Yasugi,* Momoyo Amino,† Toshiharu Suzuki,‡ Tairo Oshima,† and Akihiko Yamagishi†,[2]

**Institute of Applied Biochemistry, University of Tsukuba, Tsukuba, Ibaraki 305-8572; †Department of Molecular Biology, Tokyo University of Pharmacy and Life Science, 1432-1 Horinouchi, Hachioji, Tokyo 192-0392; and ‡Research Laboratories of Resource Utilization, Tokyo Institute of Technology, Yokohama 226-8522*

Received December 1, 2000; accepted December 29, 2000

We have performed random mutagenesis coupled with selection to isolate mutant enzymes with high catalytic activities at low temperature from thermophilic 3-isopropylmalate dehydrogenase (IPMDH) originally isolated from *Thermus thermophilus*. Five cold-adapted mutant IPMDHs with single-amino-acid substitutions were obtained and analyzed. Kinetic analysis revealed that there are two types of cold-adapted mutant IPMDH: k_{cat}-improved (improved in k_{cat}) and K_m-improved (improved in k_{cat}/K_m) types. To determine the mechanisms of cold adaptation of these mutants, thermodynamic parameters were estimated and compared with those of the *Escherichia coli* wild-type IPMDH. The ΔG_m values for Michaelis intermediate formation of the k_{cat}-improved-type enzymes were larger than that of the *T. thermophilus* wild-type IPMDH and similar to that of the *E. coli* wild-type IPMDH. The ΔG_m values of K_m-improved-type enzymes were smaller than that of the *T. thermophilus* wild-type IPMDH. Fitting of NAD^+ binding was improved in the K_m-improved-type enzymes. The two types of cold-adapted mutants employed one of the two strategies of *E. coli* wild-type IPMDH: relative destabilization of the Michaelis complex in k_{cat}-improved-type, and destabilization of the rate-limiting step in K_m-improved type mutants. Some cold-adapted mutant IPMDHs retained thermostability similar to that of the *T. thermophilus* wild-type IPMDH.

Key words: cold adaptation mechanism, 3-isopropylmalate dehydrogenase, structure–function relationship, thermodynamics, thermophilic enzyme.

Homologous enzymes adapted to different temperatures show different physical properties despite their high structural similarities. Enzymes from thermophiles show higher thermostability than their counterparts from mesophiles and psychrophiles. On the other hand, psychrophilic enzymes have lower thermostability and higher catalytic activities at low temperatures than their thermophilic counterparts. For instance, the effects of temperature on K_m for pyruvate of A_4-lactate dehydrogenase (A_4-LDH) from species adapted to different temperatures reflect the temperature of the habitat where the species were isolated (*1–3*). Although K_m tends to increase with increasing temperature, numerous studies have shown that A_4-LDH orthologues conserve K_m within a narrow range when measured at normal body temperatures isolated (*1, 4, 5*). Moreover, several structural properties have been proposed for natural psychrophilic enzymes, such as improved affinity of the ligand, distributed electrostatic interaction, increased flexibility of the domain, reduced interactions of the subunit interface, presence of long loops, reduced amount of Pro residues, and presence of a solvent-accessible hydrophobic surface area or intramolecular ion pairs (*6*).

Analysis of the sequence–structure–function relationship of homologous proteins from organisms adapted to different temperatures has provided important insights into the molecular basis of protein adaptation. A number of temperature adaptation mechanisms have been proposed. However, comparative studies of evolutionarily related proteins are hampered by the fact that many random mutations that have accumulated during divergent evolution. It is difficult to attribute adaptive mutations to certain residues against a background of many neutral substitutions.

IPMDH is an ideal model for comparing enzymatic and thermal properties. The *leu*B genes encoding IPMDHs have been cloned from various microorganisms including an extreme thermophile, *Thermus thermophilus*, and the sequences have been reported (*7–11*). The three-dimensional structure of the *T. thermophilus* IPMDH has been determined by X-ray diffraction analysis (*12*). The enzyme is a

[1] This work was supported by a grant for Evolutionary Molecular Engineering from NEDO (New Energy and Industrial Technology Development Organization) and Grants-in-Aid for Scientific Research (09558081, 10044095, 11794038) from the Ministry of Education, Science, Sports and Culture of Japan.

[2] To whom corresponding should be addressed. Tel: +81-426-76-7139, Fax: +81-426-76-7145, E-mail: yamagish@LS.toyaku.ac.jp

Abbreviations: A335V, Ala was replaced with Val at position 335; *E. coli* WT, *Escherichia coli* wild-type 3-isopropylmalate dehydrogenase; G12S, Gly was replaced with Ser at position 12; IPM, isopropylmalate; IPMDH, 3-isopropylmalate dehydrogenase; R85C, Arg was replaced with Cys at position 85; S92F, Ser was replaced with Phe at position 92; S248T, Ser was replaced with Thr at position 248; *T. th* WT, *Thermus thermophilus* wild-type 3-isopropylmalate dehydrogenase; V15I, Val was replaced with Ile at position 15; V126M, Val was replaced with Met at position 126.

dimeric protein composed of two identical subunits, each having 345 amino acid residues.

3-Isopropylmalate dehydrogenase (IPMDH, EC 1.1.1.85) catalyzes the oxidative decarboxylation of *threo*-D-3-isopropylmalate (*threo*-D-3-IPM) to 2-oxoisocaproate in the third step of the leucine biosynthetic pathway (*13*). The catalytic reaction can be summarized as:

$$\text{IPMDH-S} + \text{NAD}^+ \overset{K_m}{\longleftrightarrow} \text{IPMDH-S-NAD}^+ \overset{k_{cat}}{\longrightarrow} \text{IPMDH-P} + \text{NADH},$$

where IPMDH-S and IPMDH-P represent the IPMDH complex with the substrate IPM and the product 2-oxoisocaproate, respectively.

T. thermophilus IPMDH is homologous to the mesophilic *E. coli* IPMDH. Its melting temperature is 24°C higher than that of *E. coli* IPMDH, and its optimum temperature for specific activity is 20°C higher than that of the *E. coli* IPMDH. However, it shows little activity at mesophilic temperatures. *T. thermophilus* IPMDH shows only 52% identity in the 345 amino acid residues with *E. coli* IPMDH (*14*). It is difficult to correlate the structural difference to the difference in properties.

We have developed an isolation protocol for obtaining mutants from *T. thermophilus* IPMDH with enhanced activity at a low temperature. The protocol consists of random mutagenesis and selection. We have recently reported selection of cold-adapted mutant IPMDHs with increased catalytic activity at 40°C (*15*). Four cold-adapted mutant IPMDHs were analyzed and it found to be classifiable into two types: k_{cat}-improved type and K_m-improved type. The k_{cat}-improved-type enzymes showed an improved k_{cat} with increased K_m for coenzyme NAD^+. The K_m-improved-type enzyme showed a decreased K_m for NAD^+. Thermodynamic analysis revealed that free energy changes for binding of the k_{cat}-improved-type enzymes are enthalpy driven. However, the mechanism of cold adaptation of the K_m-improved type has not been elucidated. Because two of the three mutant IPMDHs did not have decreased thermostability, Suzuki *et al.* suggested that enhancement of catalytic activity at a low temperature does not necessarily result in a decrease in thermostability (*15*). Cold adaptation of mesophilic subtilisin BPN' is compatible with the idea of activity-thermostability incompensation (*16*). In this study, we improved the selection system for isolation of cold-adapted mutant IPMDHs. We selected cold-adapted mutant IPMDHs using a new system. We also describe the mechanisms of cold adaptation of these mutants by comparing them with those of their mesophilic counterpart, *E. coli* wild-type IPMDH (*E. coli* WT).

MATERIALS AND METHODS

Materials—*E. coli* OM17, a *leu*B-deficient strain of *E. coli* JM105, was used as a host for selection and expression of the wild-type and mutant IPMDHs (*17*). Plasmid pNV119 constructed by inserting the *T. thermophilus leu*B gene into a *Bam*HI site of plasmid pUC119 (*17*) was used for mutagenesis and expression of IPMDH. For overexpression of the recombinant *leu*B gene, *E. coli* OM17 harboring the expression plasmid was cultivated in LB medium containing 200 μM IPTG and 150 μg/ml ampicillin.

Threo-DL-3-isopropylmalate (*threo*-DL-3-IPM) was purchased from Wako Pure Chemical, NAD^+ was obtained from Oriental Yeast. Synthetic oligonucleotides were obtained from Amersham Pharmacia Biotech, Inc. Restriction endonucleases and DNA modifying enzymes were obtained from Toyobo, Takara Shuzo, and New England Biolabs. All other chemicals used were of the purest grade and commercially available.

Random Mutagenesis—Plasmid pNV119 was used as template DNA for random mutagenesis by PCR (*18*). Two synthetic oligonucleotides, 5'-GTTTTCCCAGTCACGACGTTG-3' and 5'-GAGCGGATAACAATTTCACACAGG-3', were used as primers for amplification of the *leu*B gene. PCR was carried out with 0.5 ng of template DNA in the reaction mixture containing 40 pmol of each primer, 0.2 mM concentration of each dNTP, 10 mM Tris-HCl (pH 8.3), 50 mM KCl, 1.5 mM $MgCl_2$, and 1.25 U of Gene *Taq* DNA polymerase in a total volume of 30 μl. $MnCl_2$ (0.2 mM) was added to the mixture when indicated. PCR consisted of 30 cycles of denaturation for 30 s at 95°C, annealing for 1 min at 60°C, and extension for 5 min at 72°C. The PCR product was digested with *Hin*dIII and *Eco*RI and ligated with *Hin*dIII/*Eco*RI-digested pUC119. *E. coli* OM17 was transformed with the ligate, and transformants were cultivated on LB plates supplemented with ampicillin at 37°C. The colonies were recovered from the plates using 10% glycerol, washed with 10% glycerol and suspended in the same solution. The suspension was spread on M9 minimum medium plates supplemented with ampicillin and the plates were incubated at 30°C for 3 days. Colonies that formed were checked for growth on M9 minimum medium plates at 25°C. The plasmids isolated from the colonies that grew at 25°C were used for DNA sequence analysis. The sequencing reactions were carried out using an ABI PRISM Dye Terminator Cycle Sequencing kit and AmpliTaq DNA Polymerase FS. The primers used were M13-42 (5'-GAGCGGATAACAATTTCACACAGG-3'), ATL-D (5'-TTGTGCCTCGCGATG-3'), RV-M (5'-GTTTTCCCAGTCACGACGTTG-3'), and ATL-U (5'-ATGGCGTCCACATACTGGTG-3'). The sequence was recorded on an ABI PRISM 377 DNA sequencer.

Expression and Purification of Enzymes—*E. coli* OM17 harboring a plasmid of each cold-adapted *leu*B gene was cultivated in LB medium containing ampicillin and IPTG at 37°C. Purification of the wild-type and cold-adapted IPMDHs was carried out using the procedure described previously (*19*) with minor modifications. In brief, the *E. coli* cells were disrupted by sonication, and the cell extracts were heated for 20 min at 70°C. The enzymes were purified using Butyl-Toyopearl 650s (Tosoh Corp.) and Resource Q (Pharmacia Biotech) columns, and the purified enzymes were stored at 4°C. The concentration of the enzymes was estimated based on the molar extinction coefficient of 30,400 at 280 nm (*19*).

Estimation of Kinetic and Thermodynamic Parameters—The catalytic rate was estimated based on the NAD^+ reduction by measuring the initial rate of the increase in absorbance at 340 nm with a Beckman DU7400 Spectrophotometer. The reaction was initiated by the addition of 0.6 μg of enzyme to the assay mixture [50 mM HEPES buffer (pH 8.0) containing 100 mM KCl, 5 mM $MgCl_2$, 0.4 mM DL-IPM, and 0.003–5 mM NAD^+] that had been preincubated for 5 min. The Michaelis constant (K_m) for coenzyme NAD^+ and the k_{cat} value were estimated by fitting the initial velocity data to the Michaelis-Menten equation. The

K_m value for substrate IPM was measured using assay buffers containing 1–20 μM IPM and a saturating concentration of NAD^+. The thermodynamic parameters, *i.e.*, changes in activation free energy (ΔG^*), enthalpy (ΔH^*), and entropy (ΔS^*), and changes in van't Hoff free energy (ΔG_m), enthalpy (ΔH_m) and entropy (ΔS_m) were calculated according to the relationships presented in a previous report (*20*).

CD Measurement—The wild-type and mutant IPMDHs (0.2 mg/ml) were dissolved in 20 mM phosphate buffer (pH 7.0). The circular dichroism (CD) was measured with a Jasco-J-720 Spectropolarimeter in a cell of 1-mm pathlength. Loss of the secondary structure in the wild-type and mutant IPMDHs was monitored by recording the CD signal at 222 nm as a function of temperature. The temperature was increased at a rate of 1°C/min.

RESULTS

Selection of Cold-adapted Mutant IPMDHs—Error-prone PCR was carried out with and without 0.2 mM $MnCl_2$. Sequence analysis of randomly selected clones of the libraries revealed that the clones obtained by the PCR with and without $MnCl_2$, respectively, contained substitutions of about two or three and one base-pair per gene. These were used for selection on M9 minimum medium plates. Sixty and 64 colonies were isolated from the two plasmid libraries of 1.1×10^5 and 7.9×10^4 transformants, respectively, within 3 days at 30°C. The colonies were tested for growth on M9 minimum medium plates at 25°C. All of the clones isolated at 30°C grew at 25°C. Eighty randomly selected clones were sequenced, and 49 clones were found to have either single or multiple amino-acid substitutions (Table I). The remaining clones did not carry any base substitutions in the coding region of the *leu*B gene. These strains were selected probably because the expression of the *leu*B gene was enhanced. Among the 13 single-amino-acid mutants, 5 out of 7 randomly selected mutants showed a higher ratio of 40/60°C activity than *T. thermophilus* wild-type IPMDH (*T. th* WT) and were used for further analysis. E161K and K178T were not analyzed further because the activity ratio 40/60°C was lower than that of *T. th* WT.

Temperature Dependence of Specific Activity—*T. th* WT and mutant IPMDHs and *E. coli* WT were purified to homogeneity as determined by results of sodium dodecyl sulfate polyacrylamide gel electrophoresis (data not shown).

The specific activity of the selected mutant IPMDHs, *T. th* WT, and *E. coli* WT was determined in the temperature range of 30–95°C (Fig. 1). Mutants R85C and S248T had higher specific activity than *T. th* WT but much lower activity than *E. coli* WT in the temperature range of 30–60°C. G12S and K21T showed similar specific activity profiles to *T. th* WT. A335V had a lower specific activity than *T. th* WT in the temperature range examined.

Kinetic Parameters—The kinetic parameters of selected mutant IPMDHs, *T. th* WT, and *E. coli* WT were determined at 30 and 60°C (Table II). The selected mutant IPMDHs showed improved activity at 30°C compared with that of *T. th* WT. The k_{cat} was between 0.86- and 6.80-fold, and K_m for NAD^+ was between 0.42- and 25.1-fold that of the *T. th* WT. K_m for IPM was between 0.30- and 2.83-fold that of the wild-type. The mutant IPMDHs could be classified into two types, similarly to the previously selected mutant IPMDHs (*15*). R85C and S248T showed an increased k_{cat} (k_{cat}-improved type), and G12S, K21T, and A335V showed an increased k_{cat}/K_m (K_m-improved type). Improvements in these parameters were less significant at higher temperatures. These mutant IPMDHs can be called cold-adapted mutant enzymes as defined by Feller *et al.* (*21*).

Thermodynamic Parameters—The thermodynamic parameters of the selected mutant IPMDHs, *T. th* WT, and *E. coli* WT were estimated from the temperature dependence of the kinetic parameters (Table III). These parameters clearly show two types of mutant enzyme.

In the k_{cat}-improved-type enzymes (R85C and S248T), the free energy change for NAD^+ binding estimated from K_m (ΔG_m) increased and became similar to that of *E. coli* WT. Moreover, the activation free energy change for catalytic activity estimated from k_{cat} (ΔG^*) was reduced to a

TABLE I. **Amino acid substitutions of sequenced clones.**

Error-prone PCR without $MnCl_2$		Error-prone PCR with 0.2 mM $MnCl_2$	
Amino acid substitution	Number of clones	Amino acid substitutions	Number of clones
A4V	1	V15G+V67A+R85C	1
G12S	1	T16A+E161K	2
K21T	1	T16A+V199A	2
V108A	2	R85C	6
F140L	1	R85C+I130T	1
G141R	1	R85C+V199M	1
M221V	1	V128A+E161K	1
V249A	1	E161K	9
A335V	1	E161K+V199A	1
No substitution	25	E161K+S248T	2
		K178E	1
		F194L+S248T	1
		S248T	7
		S248T+A314P	1
		No substitution	6
Total	35	Total	45

TABLE II. **Kinetic parameters of enzymatic reactions of cold-adapted mutant, *T. thermophilus* wild-type, and *E. coli* wild-type IPMDHs.**

Enzyme	K_mIPM (μM)		K_mNAD (μM)		k_{cat} (s^{-1})		k_{cat}/K_m (s^{-1} μM^{-1})	
	30°C	60°C	30°C	60°C	30°C	60°C	30°C	60°C
T. th WT	0.9 (1.00)	2.6 (1.00)	9.2 (1.00)	134.2 (1.00)	0.7 (1.00)	25.5 (1.00)	0.076 (1.00)	0.190 (1.00)
G12S	0.3 (0.33)	1.5 (0.58)	4.5 (0.49)	82.2 (0.61)	0.9 (1.29)	20.5 (0.80)	0.200 (2.63)	0.249 (1.31)
K21T	1.7 (1.89)	3.8 (1.46)	7.8 (0.85)	111.4 (0.83)	1.0 (1.43)	19.9 (0.78)	0.128 (1.68)	0.179 (0.94)
R85C	2.5 (2.78)	4.4 (1.69)	93.7 (10.18)	454.1 (3.38)	4.8 (6.86)	36.4 (1.43)	0.051 (0.67)	0.080 (0.42)
S248T	0.6 (0.67)	3.4 (1.31)	230.8 (25.09)	990.5 (7.38)	4.0 (5.71)	33.1 (1.30)	0.017 (0.23)	0.033 (0.18)
A335V	0.4 (0.44)	0.8 (0.31)	3.9 (0.42)	60.5 (0.45)	0.8 (1.14)	14.0 (0.55)	0.205 (2.70)	0.231 (1.22)
E. coli WT	2.7 (3.00)	9.1 (3.50)	117.4 (12.76)	864.1 (6.44)	39.8 (56.86)	203.9 (8.00)	0.339 (4.46)	0.236 (1.24)

Values relative to those of *T. thermophilus* wild-type IPMDH are indicated in parentheses.

similar degree to the change in ΔG_m ($\Delta\Delta G_m$). The van't Hoff plot (Fig. 2a) of the k_{cat}-improved-type enzymes shows lower slopes than that of *T. th* WT, indicating increased ΔH_m compared with that of *T. th* WT. This increase in ΔH_m caused the increase in ΔG_m in the k_{cat}-improved-type enzymes. The Arrhenius plots (Fig. 2b) show that ΔH^* also decreased in this type of mutant. ΔH^* and $T\Delta S^*$ showed compensatory changes in all the mutant enzymes. In particular, the $T\Delta S^*$ of the k_{cat}-improved enzymes become negative and approached that of *E. coli* WT.

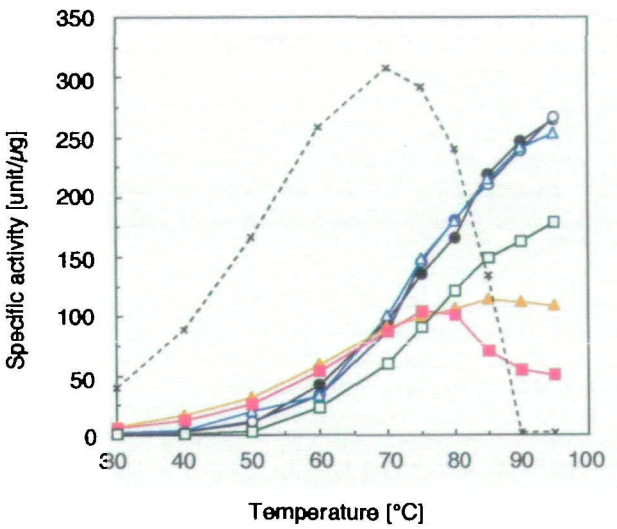

Fig. 1. **Temperature dependence of specific activities of cold-adapted mutants of *T. thermophilus* wild-type, and *E. coli* wild-type.** ●, *T. th* WT; ×, *E. coli* WT; ○, G12S; △, K21T; ▲, R85C; ■, S248T; and □, A335V.

In the K_m-improved enzymes (G12S, K21T, and A335V), ΔG_m decreased (Table III). ΔG^* slightly decreased in G12S and K21T, and slightly increased in A335V compared with that of *T. th* WT. The slope of the van't Hoff plot (Fig. 2a) of the K_m-improved enzymes decreased slightly, and ΔH_m was lower than that of *T. th* WT. The change in ΔG_m was caused by the decrease in ΔH_m.

Thermostability—The apparent melting temperatures estimated to be the midpoint of denaturation (T_m) estimated from CD at 222 nm are summarized in Table IV. Small changes in thermostability were detected in the selected mutant IPMDHs, especially G12S and K21T compared with that of *T. th* WT.

DISCUSSION

Selection of Cold-Adapted Strains of E. coli—In our previous report we developed a genome-integration vector for *leu*B gene in *E. coli*. We have integrated the *T. thermophilus leu*B gene at the *leu*B locus of the *E. coli* genome with the vector. *E. coli* strains with cold-adapted *T. thermophilus leu*B genes were selected at 40°C. Four of five *leu*B sequences analyzed encoded cold-adapted IPMDHs.

In this work, we have used a plasmid expression vector and a *leu*B-deficient *E. coli* strain. The *E. coli* strain harboring the wild-type *T. thermophilus leu*B gene could grow at 40°C, probably because of the higher expression of the gene with the plasmid vector than with the integration vector. Cold-adapted mutant strains were selected at 30°C. A higher number of strains selected with plasmid vector system harbored the *leu*B genes with no substitution, especially with PCR condition for higher fidelity. However, the

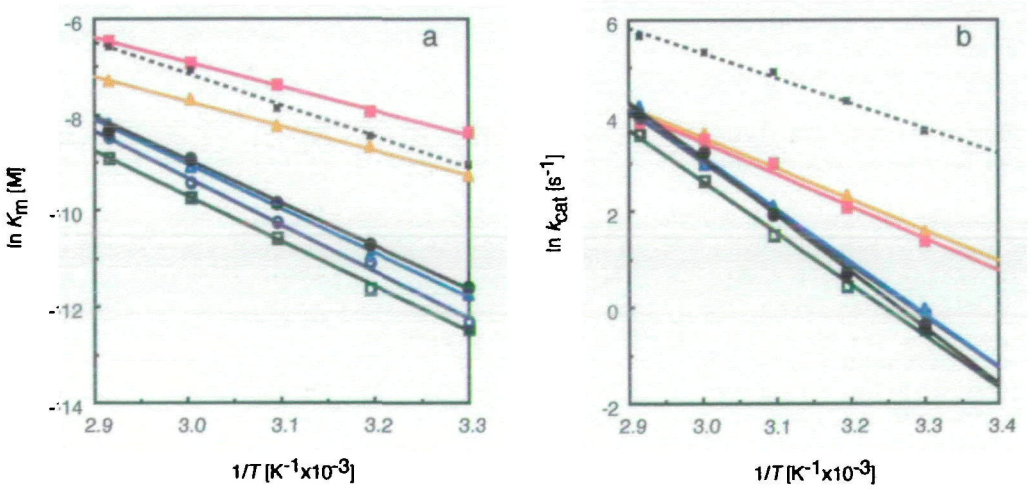

Fig. 2. **van't Hoff plots of the K_m for NAD$^+$ (a) and Arrhenius plots of the k_{cat} (b) of cold-adapted mutants of *T. thermophilus* wild-type, and *E. coli* wild-type.** ●, *T. th* WT; ×, *E. coli* WT; ○, G12S; △, K21T; ▲, R85C; ■, S248T; and □, A335V.

TABLE III. **Thermodynamic parameters of enzymatic reaction of cold-adapted mutant, *T. thermophilus* wild-type, and *E. coli* wild-type IPMDHs (30°C).**

Enzyme	ΔG_m (kcal/mol)	$\Delta\Delta G_m$ (kcal/mol)	ΔH_m (kcal/mol)	$\Delta\Delta H_m$ (kcal/mol)	$T\Delta S_m$ (kcal/mol)	$T\Delta\Delta S_m$ (kcal/mol)	ΔG^* (kcal/mol)	$\Delta\Delta G^*$ (kcal/mol)	ΔH^* (kcal/mol)	$\Delta\Delta H^*$ (kcal/mol)	$T\Delta S^*$ (kcal/mol)	$T\Delta\Delta S^*$ (kcal/mol)
T. th WT	−6.98	0.00	−17.90	0.00	−10.89	0.00	17.96	0.00	22.65	0.00	4.65	0.00
G12S	−7.41	−0.43	−19.36	−1.46	−12.00	−1.11	17.81	−0.15	20.64	−2.01	2.79	−1.86
K21T	−7.08	−0.10	−18.50	−0.60	−11.38	−0.49	17.76	−0.20	21.01	−1.64	3.19	−1.46
R85C	−5.58	1.40	−10.20	7.70	−4.63	6.26	16.80	−1.16	12.12	−10.53	−4.65	−9.30
S248T	−5.04	1.94	−10.06	7.84	−4.99	5.90	16.91	−1.05	12.60	−10.05	−4.27	−8.92
A335V	−7.50	−0.52	−18.63	−0.73	−11.10	−0.21	18.02	0.06	20.65	−2.00	2.56	−2.09
E. coli WT	−5.45	1.53	−13.05	4.85	−7.57	3.32	15.53	−2.43	10.42	−12.23	−5.09	−9.74

TABLE IV. **Thermostability of cold adapted mutant, *T. thermophilus* wild-type, and *E. coli* wild-type IPMDHs.**

Enzyme	Type	T_m (°C)	ΔT_m (°C)
T. th WT		87.0	(0)
G12S	K_m-improved	86.0	(−1.0)
K21T	K_m-improved	86.5	(−0.5)
R85C	k_{cat}-improved	83.0	(−4.0)
S248T	k_{cat}-improved	84.5	(−2.5)
A335V	K_m-improved	85.0	(−2.0)
E. coli WT*		63.0	(−24.0)

*Wallon, G. *et al.* (1997) *Biochim. Biophys. Acta* **1337**, 105–112.

analysis of the mutant genes is easier with the plasmid-vector system.

Temperature Dependence of Activity of IPMDHs—Two k_{cat}-improved IPMDHs showed higher specific activity than *T. th* WT at lower temperatures. The decrease of the specific activity of k_{cat}-improved IPMDHs at higher temperatures can be ascribed to the increase of K_m value for NAD^+ at higher temperatures.

K_m values for NAD^+ and k_{cat} value were estimated at temperatures between 30 and 70°C. Thermodynamic parameters were estimated from the temperature dependence of K_m and k_{cat} values for cold-adapted IPMDHs, *T. th* WT and *E. coli* WT. The results are summarized in Table III and schematically represented in Fig. 3.

Cold Adaptation of the k_{cat}-Improved Type—Figure 3a shows the free energy profiles relative to the initial state along the reaction coordinate for the cold-adapted mutant IPMDHs, *T. th* WT, and *E. coli* WT at 30°C. The free energy level at the Michaelis complex state (IPMDH-S-NAD^+) relative to the initial state increased in the k_{cat}-improved mutants (R85C and S248T) and was similar to that of *E. coli* WT. Figure 3a clearly shows that the free energy level of the Michaelis complex state relative to the initial state increased to a similar level to that of *E. coli* WT. This increase mainly enhances the catalytic reaction in the k_{cat}-improved mutants. The enthalpy and entropy profiles along the reaction coordinate are also shown in Fig. 3, b and c, respectively. These figures illustrate that the shift in free energy level of the Michaelis complex state relative to the initial state is induced by the increase in the enthalpy level of the Michaelis complex state, although the change is partially compensated by a shift in the entropy level of this state in the k_{cat}-improved enzymes. These thermodynamic characteristics are similar to those of the three k_{cat}-improved enzymes reported a previously, though we have not compared the characteristics with those of *E. coli* WT (*15*).

Although the difference between the Michaelis complex state and transition ((IPMDH-S-NAD^+)*) state decreased in the k_{cat}-improved enzymes compared with that of *T. th* WT, the free energy level of the transition state of the former was higher than that of the latter. The free energy changes for the entire catalytic reaction were still smaller in *E. coli* WT than in the k_{cat}-improved types.

Cold Adaptation of K_m-Improved Type—In the K_m-improved enzymes (G12S, K21T, and A335V), the k_{cat}/K_m value increased despite a similar or lower specific activity than that in *T. th* WT. Lower K_m values enable a higher reaction rate under the condition unsaturated with coenzyme NAD^+. The intracellular concentrations of NAD^+ are not expected to be so high as to saturate the enzyme reaction rate. Because NAD^+ is involved in many metabolic reactions, its concentration is not expected to change with a change in the rate of the leucine biosynthesis.

The K_m-improved enzymes showed a lower free energy level of the Michaelis complex state than *T. th* WT. The levels of enthalpy and entropy of the Michaelis complex state relative to the initial state also decreased in these enzymes (Fig. 3, b and c). Because the change in $T\Delta S_m$ was smaller than the change in ΔH_m, ΔG_m ($=\Delta H_m - T\Delta S_m$) decreased in these mutants. Accordingly, the decrease in the free energy level of the Michaelis complex state relative to the initial state in the K_m-improved enzymes at a low temperature was induced by the decrease in the enthalpy level of the Michaelis complex state. Although ΔG^* did not decrease significantly (it was increased in one of them) compared with that of *T. th* WT, free energy levels of the transition state of the K_m-improved enzymes were lower than that of *T. th* WT and become closer to that of *E. coli* WT because of the decrease in ΔG_m. Accordingly, the enhanced activity of the K_m-improved enzymes at low temperature can be ascribed to the closeness of energy levels between the initial state and the transition state. The free energy level of the transition state relative to the initial state in K_m-improved enzymes was closer to that of *E. coli* WT.

Comparison with Natural Psychrophilic Enzymes—As described by Feller *et al.* (1996), natural psychrophilic enzymes have three general characteristics in common in contrast to their mesophilic or thermophilic counterparts:

- A downward shift in their apparent optimum temperature for activity.
- A higher k_{cat} or k_{cat}/K_m at 0–30°C.
- Rapid denaturation at moderate temperature.

These characteristics were observed in various enzymes such as α-amylase, subtilisin, LDH, triose phosphate isomerase, malate dehydrogenase, and lipase, as well as in natural IPMDHs (*20–24*). Our cold-adapted mutant IPMDHs exhibited the second characteristic.

It has been shown that the activation energy of cold-adapted enzymes is lower than that of thermophilic enzymes (*25–28*). Low activation energy indicates that a catalytic reaction is relatively temperature-independent. The low-temperature dependence enables psychrophilic enzymes to reduce variability in their reaction rate that could result from environmental temperature fluctuations. The mechanism of cold adaptation particularly in the k_{cat}-improved enzymes was similar to that of natural psychrophilic enzymes that often experience large temperature changes in their surroundings diurnally and/or seasonally, whose rates of enzymatic reactions have to be relatively stable.

Although detailed thermodynamic parameters have not been analyzed, higher enzymatic activity at low temperature and low-temperature dependence of enzymatic activity have been reported in cold-adapted mutants of subtilisin BPN' and indolglycerol phosphate synthase (*29–31*). In these mutant enzymes, a cold-adaptation mechanism similar to that in the natural psychrophilic enzymes (k_{cat}-improved type) is expected to enhance the enzymatic activity at low temperatures. The mechanism of enhanced activity at low temperature that was observed in the K_m-improved mutants has not been reported in any psychrophilic and cold-adapted mutant enzymes. In our cold-adaptation experiments, two types of cold-adapted mutants employed one of the two strategies of *E. coli* wild-type IPMDH: desta-

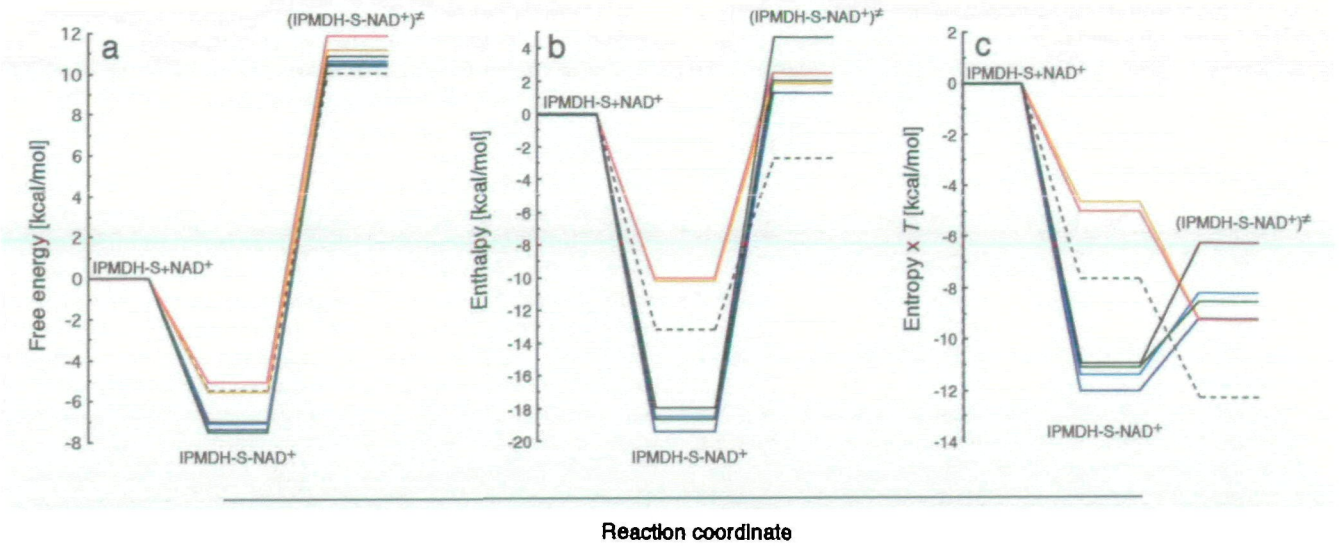

Fig. 3. **Free energy (a), enthalpy(b), and entropy(c) profiles relative to the initial state along the reaction coordinate for the wild-type and cold-adapted mutants of *T. thermophilus* wild-type, and *E. coli* wild-type.** Black line, *T. th* WT; broken black line, *E. coli* WT; blue line, G12S; cyan line, K21T; yellow line, R85C; magenta line, S248T; and green line, A335V.

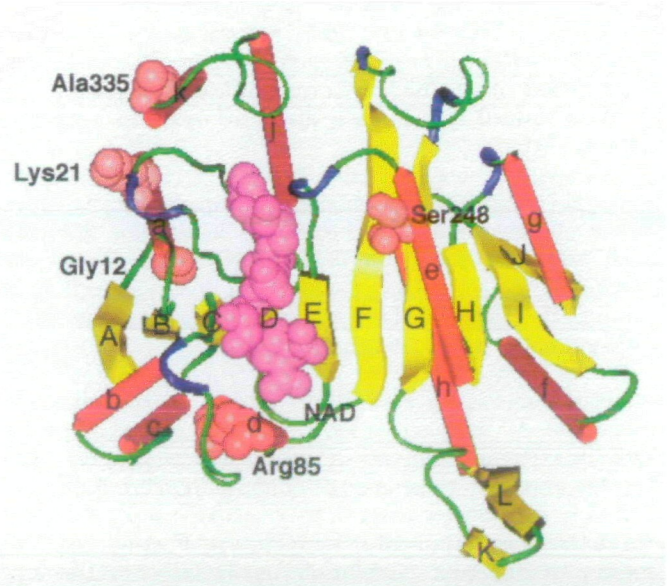

Fig. 4. **Location of substituted residues on the thread model of *T. thermophilus* IPMDH.** The structure of co-crystallized *T. thermophilus* IPMDH with NAD+ (PDB code: 1HEX, Ref. *37*) was used for the figure. The figure was drawn using Insight II (Molecular Simulations Inc.). Red cylinders, α-helices; yellow arrows, β-strands; blue arrows, turn; green lines, random coil; purple spacefills, coenzyme NAD+; red spacefills, substituted residues in cold-adapted mutant IPMDHs.

bilization of Michaelis complex in k_{cat}-improved mutants, and destabilization of the rate-limiting step in K_m-improved mutants relative to the initial state.

Thermostability—It has been suggested that low catalytic rates could be due to thermophilic enzymes being more rigid at mesophilic temperatures (*32*). However, in G12S and K21T, T_m did not change significantly compared with that of *T. th* WT. The previous analysis on cold-adapted mutant IPMDHs, S92F (K_m-improved type) and V126M (k_{cat}-improved type), which retain the original thermostability, indicated that there is not an inverse relationship between activity and thermostability (*15*). A number of studies of mutant IPMDHs (*14*, *17*, *33–35*) have revealed residues which contribute to the thermostability of *T. thermophilus* IPMDH. In addition, several stabilized mutant IPMDHs selected by evolutionary engineering techniques using *T. thermophilus* had mutations in interdomain hydrophobic contact regions, which also supports the importance of interdomain interaction (*36*). None of these mutants exhibited an inverse relationship between thermostability and catalytic activity. Point-mutation studies of triosephosphate isomerase (*37*), subtilisin (*38*), LDH (*1*, *23*), and β-glucosidase A (*39*) showed that kinetic properties are not correlated with thermostability. These studies, like ours, showed additional examples that thermostability and efficient catalytic activity at low temperature are not physical trade-off requirements, and loss of thermostability of natural psychrophilic enzymes can be due to a random genetic drift (*5*, *22*, *23*, *40–42*).

Structure Comparison—Comparison of the sequences of the cold-adapted mutant IPMDHs with those of the homologous IPMDHs revealed that none of the amino acids in the cold-adapted mutants were similar to those at the corresponding positions in mesophilic counterparts. Arg85 and Ser248 are highly conserved, and Gly12 is perfectly conserved in the mesophilic IPMDHs used in the comparison. A mutation site previously reported to be Val15 (*15*) was also conserved. It is possible to enhance enzymatic activity by substituting the conserved residues in IPMDH. The main factor in increasing the activity of the k_{cat}-improved enzymes (R85C and S248T) at low temperature is considered to be the modification of the NAD+-binding site with the mutation and reduction in the affinity of NAD+, as discussed in a previous work (*15*). Dean *et al.* (*43*) have reported that the kinetic mechanism of *E. coli* isocitrate dehydrogenase (ICDH) is highly similar to the structural and reaction mechanisms of *T. thermophilus* IPMDH. The study indicated that the oxidative decarboxylation step is quite rapid (1,700 s^{-1}) compared with substrate and coenzyme

release (84.5 s^{-1}), indicating that the release step is rate-limiting for the catalytic reaction. The reduced affinity of NAD^+ was also expected to reduce the NADH affinity. Accordingly, the release of the product must be facilitated by the amino acid substitution in the k_{cat}-improved mutants.

The substituted residues in the cold-adapted mutant IPMDHs are shown in Fig. 4. Arg85 is located in the N-terminus of α-helix d, which interacts with the nicotinamide ring of NAD^+ (*12*). Arg85 is exposed to solvent and is close to the position where the residue is able to interact with Glu193′ (′ indicates a residue in another subunit) in the closed form. This intersubunit interaction may be lost as a result of the amino acid substitution at position 85,thereby destabilizing the closed form. Because the domain-movement from open to closed is expected to be relevant to the binding of substrate and coenzyme, the mutation at position 85 is expected to affect the binding of ligands.

Ser248 is located at the other side of the active site cleft of the IPMDH molecule, and Asp241 and Asp245 near Ser248 are concerned with IPM (*12*). Arg104 that interacts with IPM is also in the vicinity (*12*). Introducing one methyl group to the residue at position 248 is expected to cause subtle changes in the fitting of these residues with the substrate and coenzyme. S248T is also expected to affect the position of Val272 which is located at the root of loop 272–286. This loop contains the NAD^+ recognition residues His273, Ala276, Asp278, and Asn286 (*44*). The movement of this loop may influence the affinity with NAD^+ in this mutant.

On the other hand, in the K_m-improved type enzymes (G12S, K21T, and A335V), the NAD^+ binding was improved by the amino acid substitutions. In *T. th* WT, the adenine moiety of NAD^+ constructs hydrophobic contacts with side chains of Ile11, Val15, Leu254, Gly255, Ile279, and Asp326 (*45*). Residue Gly12 is located next to Val15 on the α-helix a, which is involved in NAD^+ binding. Gly12 was replaced with a larger residue Ser. Ser12 protrudes toward Pro7 and Ser71, and causes conformational change of α-helix a and β-strands B and C. The shift could be distributed over the molecule *via* the β-sheet, which may be a reason for the increased affinity with IPM and NAD^+.

Lys21 and Ala335 are located in α-helices a and k, respectively, which run parallel to each other. Lys21 appears to interact with Glu334 electrostatically and to stabilize the arrangement of these helices. This interaction is lost in K21T, resulting in the shift of α-helix a. This may affect the conformation of the NAD^+-binding pocket. A335V is also expected to cause rearrangement of these helices by introducing a bulky side chain. In these mutants, the conformation of bound NAD^+ may be closer to that in the transition state than in *T. th* WT, and a chemical reaction may be facilitated. Subtle structural changes in ICDH are reported to play substantial roles in enhancing the catalytic power of the enzyme (*46*). Therefore, optimizing the NAD^+ binding with IPMDH may stabilize the NAD^+ into a conformation required for its transition state when the enzyme is in a closed form. This indicates that subtle conformational change caused by a single mutation is sufficient to improve the catalytic activity of cold-adapted mutant IPMDHs.

The CD spectra of the cold-adapted mutant IPMDHs were not significantly different from that of *T. th* WT (data not shown). This indicates that there is little difference in the overall structure between the enzymes, suggesting that these mutations which cause the temperature-dependent increase in activity are not linked to large changes in the secondary structure of the enzyme.

Amino acid substitution outside the active site can alter the enthalpy and entropy changes for binding and for catalysis. These effects play a critical role in the improvement of k_{cat} and K_m. This suggests that optimization of the conformation of ligand-binding pockets is an efficient way of designing enzymes with improved activity at low temperature by single mutations, although rational design is still difficult.

REFERENCES

1. Holland, L.Z., McFall-Ngai, M., and Somero, G.N. (1997) Evolution of lactate dehydrogenase-A homologs of barracuda fishes (genus *Sphyraena*) from different thermal environments: differences in kinetic properties and thermal stability are due to amino acid substitutions outside the active site. *Biochemistry* **36**, 3207–3215
2. Ozernyuk, N.D., Klyachko, O.S., and Polosukhina, E.S. (1994) Acclimination temperature affects the functional and structural properties of lactate dehydrogenase from fish (*Musgurnus fossilis*) skeletal muscles. *Comp. Biochem. Physiol.* **107B**, 141–145
3. Somero, G.N. and Siebenaller, J.F. (1979) Inefficient lactate dehydrogenase of deep-sea fishes. *Nature* **282**, 100–102
4. Fields, P.A. and Somero, G.N. (1998) Hot spots in cold adaptation: localized increases in conformational flexibility in lactate dehydrogenase A_4 orthologs of Antarctic notothenioid fishes. *Proc. Natl. Acad. Sci. USA* **95**, 11476–11481
5. Somero, G.N. (1995) Proteins and temperature. *Annu. Rev. Physiol.* **57**, 43–68
6. Russell, R.J., Gerike, U., Danson, M.J., Hough, D.W., and Taylor, G.L. (1998) Structure adaptation of the cold-active citrate synthase from an antarctic bacterium. *Structure* **6**, 351–361
7. Andreadis, A. and Rosenthal, E.R. (1992) The nucleotide sequence of *leu*B from *Salmonella typhimurium*. *Biochim. Biophys. Acta* **1129**, 228–230
8. Andreadis, A., Hsu, Y.-P., Hermodson, M., Kohlhaw, G., and Schimmel, P. (1984) Yeast LEU2 Repression of mRNA levels by leucine and primary structure of the gene product. *J. Biol. Chem.* **259**, 8059–8062
9. Imai, R., Sekiguchi, T., Nosoh, Y., and Tsuda, K. (1987) The nucleotide sequence of 3-isopropylmalate dehydrogenase gene from *Bacillus subtilis*. *Nucleic Acids Res.* **15**, 4988
10. Sakai, Y. and Tani, Y. (1992) Directed mutagenesis in an asporogenous methylotrophic yeast: cloning, sequencing, and one-step gene disruption of the 3-isopropylmalate dehydrogenase gene (LEU2) of *Candida boidinii* to derive doubly auxotrophic marker strains. *J. Bacteriol.* **174**, 5988–5993
11. Kirino, H. and Oshima, T. (1991) Molecular cloning and nucleotide sequence of 3-isopropylmalate dehydrogenase gene (*leu*B) from an extreme thermophile, *Thermus aquaticus* YT-1. *J. Biochem.* **109**, 852–857
12. Imada, K., Sato, M., Tanaka, N., Katsube, Y., Matsuura, Y., Oshima, T., (1991) Three-dimensional structure of a highly thermostable enzyme, 3-isopropylmalate dehydrogenase of *Thermus thermophilus* at 2.2 Å resolution. *J. Mol. Biol.* **222**, 725–738
13. Pirrung, M.C., Han, H., and Nunn, D.S. (1994) Kinetic mechanism and reaction pathway of *Thermus thermophilus* isopropylmalate dehydrogenase. *J. Org. Chem.* **59**, 2423–2429
14. Kirino, H., Aoki, M., Aoshima, M., Hayashi, Y., Ohba, M., Yamagishi, A., Wakagi, T., and Oshima, T. (1994) Hydrophobic interaction at the subunit interface contributes to the thermostability of 3-isopropylmalate dehydrogenase from an extreme thermophile, *Thermus thermophilus*. *Eur. J. Biochem.* **220**, 275–281
15. Suzuki, T., Yasugi, M., Arisaka, F., Yamagishi, A., and Oshima,

T. (2001) Adaptation of a thermophilic enzyme, 3-isopropylmalate dehydrogenase, to low temperatures. *Protein Eng.* **14**, in press
16. Taguchi, S., Ozaki, A., Nonaka, T., Mitsui, Y., and Momose, H. (1999) A cold-adapted protease engineered by experimental evolution system. *J. Biochem.* **126**, 689–693
17. Tamakoshi, M., Yamagishi, A., and Oshima, T. (1995) Screening of stable proteins in an extreme thermophile, *Thermus thermophilus*. *Mol. Microbiol.* **16**, 1031–1036
18. Shibata, H., Kato, H., and Oda, J. (1998) Random mutagenesis on the *Pseudomonas* lipase activator protein, *LipB*: exploring amino acid residues required for its function. *Protein Eng.* **11**, 467–472
19. Yamada, T., Akutsu, N., Miyazaki, K., Kakinuma, K., Yoshida, M., and Oshima, T. (1990) Purification, catalytic properties, and thermal stability of threo-Ds-3-isopropylmalate dehydrogenase coded by *leu*B gene from an extreme thermophile, *Thermus thermophilus* strain HB8. *J. Biochem.* **108**, 449–456
20. Feller, G. and Gerday, C. (1997) Psychrophilic enzymes: molecular basis of cold adaptation. *Cell. Mol. Life Sci.* **53**, 830–841
21. Feller, G., Narinx, E., Arpigny, J.L., Aittaleb, M., Baise, E., Genicot, S., and Gerday, C. (1996) Enzymes from psychrophilic organisms. *FEMS Microbiol. Rev.* **18**, 189–202
22. Gerday, C., Aittaleb, M., Arpigny, J.L., Baise, E., Chessa, J.-P., Garsoux, G., Petrescu, I., and Feller, G. (1997) Psychrophilic enzymes: a thermodynamic challenge. *Biochim. Biophys. Acta* **1342**, 119–131
23. Fields, P.A. and Somero, G.N. (1997) Amino acid sequence differences cannot fully explain interspecific variation in thermal sensitivities of gobiid fish A_4-lactate dehydrogenases (A_4-LDHs). *J. Exp. Biol.* **200**, 1839–1850
24. Kohl, L., Callens, M., Wierenga, R.K., Opperdoes, F.R., and Michels, P.A.M. (1994) Triose-phosphate isomerase of *Leishmania mexicana mexicana*. *Eur. J. Biochem.* **220**, 331–338
25. Borgmann, U. and Moon, T.W. (1975) A comparison of lactate dehydrogenases from an ectothermic and an endothermic animal. *Can. J. Biochem.* **53**, 998–1004
26. Borgmann, U., Laidler, K.J., and Moon, T.W. (1975) Kinetics and thermodynamics of lactate dehydrogenases from beef heart, beef muscle, and flounder muscle. *Can. J. Biochem.* **53**, 1196–1206
27. Low, P.S., Bada, J.L., and Somero, G.N. (1973) Temperature adaptation of enzymes: roles of the free energy, the enthalpy, and the entropy of activation. *Proc. Nat. Acad. Sci. USA* **70**, 430–432
28. Thomas, T. and Cavicchioli, R. (2000) Effect of temperature on stability and activity of elongation factor 2 proteins from Antarctic and thermophilic methanogens. *J. Bacteriol.* **182**, 1328–1332
29. Kano, H., Taguchi, S., and Momose, H. (1997) Cold adaptation of a mesophilic serine protease, subtilisin, by *in virto* random mutagenesis. *Appl. Microbiol. Biotechnol.* **47**, 46–51
30. Merz, A., Yee, M.-C., Szadkowski, H., Pappenberber, G., Crameri, A., Stemmer, W.P.C., Yanofsky, C., and Kirschner, K. (2000) Improving the catalytic activity of a thermophilic enzyme at low temperatures. *Biochemistry* **39**, 880–889
31. Taguchi, S., Ozaki, A., and Momose, H. (1998) Engineering of a cold-adapted protease by sequential random mutagenesis and a screening system. *Appl. Environ. Microbiol.* **64**, 492–495
32. Wrba, A., Schweiger, A., Schultes, V., Jaenicke, R., and Zavodszky, P. (1990) Extremely thermostable D-glyceraldehyde-3-phosphate dehydrogenase from the eubacterium *Thermotoga maritima*. *Biochemistry* **29**, 7584–7592
33. Numata, K., Muro, M., Akutsu, N., Nosoh, Y., Yamagishi, A., and Oshima, T. (1995) Thermal stability of chimeric isopropylmalate dehydrogenase genes constructed from a thermophile and a mesophile. *Protein Eng.* **8**, 39–43
34. Kotsuka, T., Akanuma, S., Tomuro, M., Yamagishi, A., and Oshima, T. (1996) Further stabilization of 3-isopropylmalate dehydrogenase of an extreme thrmophile, *Thermus thermophilus*, by a suppressor mutation method. *J. Bacteriol.* **178**, 723–727
35. Akanuma, S., Yamagishi, A., Tanaka, N., and Oshima, T. (1999) Further improvement of the thermal stability of a partially stabilized *Bacillus subtilis* 3-isopropylmalate dehydrogenase variant by random and site-directed mutagenesis. *Eur. J. Biochem.* **260**, 499–504
36. Akanuma, S., Qu, C., Yamagishi, A., Tanaka, N., and Oshima, T. (1997) Effect of polar side chains at position 172 on thermal stability of 3-isopropylmalate dehydrogenase from *Thermus thermophilus*. *FEBS Lett.* **410**, 141–144
37. Williams, J.C., Zeelen, J.P., Neubauer, G., Vriend, G., Backmann, J., Michels, P.A.M., Lambeir, A.-M., and Wierenga, R.K. (1999) Structural and mutagenesis studies of leishmania triosephosphate isomerase: a point mutation can convert a mesophilic enzyme into a superstable enzyme without losing catalytic power. *Protein Eng.* **12**, 243–250
38. Narinx, E., Baise, E., and Gerday, C. (1997) Subtilisin from psychrophilic antactic bacteria: characterization and site-directed mutagenesis of residues possibly involved in the adaptation to cold. *Protein Eng.* **10**, 1271–1279
39. Lopez-Camacho, C., Salgado, J., Lequerica, J.L., Madarro, A., Ballestar, E., Franco, L., and Polaina, J. (1996) Amino acid substitutions enhancing thermostability of *Bacillus polymyxa* β-glucosidase A. *Biochem. J.* **314**, 833–838
40. Miyazaki, K., Wintrode, P.L., Grayling, R.A., Rubingh, D.N., and Arnold, F.H. (2000) Directed evolution study of temperature adaptation in a psychrophilic enzyme. *J. Mol. Biol.* **297**, 1015–1026
41. Vihinen, M. (1987) Relationship of protein flexibility to thermostability. *Protein Eng.* **1**, 477–480
42. Hayashi-Iwasaki, Y., Numata, K., Yamagishi, A., Yutani, K., Sakurai, M., Tanaka, N., and Oshima, T. (1996) A stable intermediate in the thermal unfolding process of a chimeric 3-isopropylmalate dehydrogenase between a thermophilic and a mesophilic enzymes. *Protein Sci.* **5**, 511–516
43. Dean, A.M. and Koshland, D.E. Jr. (1993) Kinetic mechanism of *Escherichia coli* isocitrate dehydrogenase. *Biochemistry* **32**, 9302–9309
44. Kadono, S., Sakurai, M., Moriyama, H., Sato, M., Hayashi, Y., Oshima, T., and Tanaka, N. (1995) Ligand-induced changes in the conformation of 3-isopropylmalate dehydrogenase from *Thermus thermophilus*. *J. Biochem.* **118**, 745–752
45. Hurley, J.H. and Dean, A.M. (1994) Structure of 3-isopropylmalate dehydrogenase in complex with NAD^+: ligand-induced loop closing and mechanism for cofactor specificity. *Structure* **2**, 1007–1016
46. Mesecar, A.D., Stoddard, B.L., and Koshland, D.E. Jr. (1997) Orbital steering in the catalytic power of enzymes: small structural changes with large catalytic consequences. *Science* **227**, 202–206